Dynamic analysis of an offshore jacket platform with a tuned mass damper under the seismic and ice loads

R.K. Sharma[1a], V. Domala[2b] and R. Sharma[*3]

[1]L&T-Valdel Engineering Limited, India
[2]RIMSE, CADIT Lab, Seoul National University, Republic of Korea
[3]Design and Simulation Laboratory, Department of Ocean Engineering, IIT Madras, India

Abstract. Herein, we present numerical simulation based model to study the use of a 'Tuned Mass Damper (TMD)' - particularly spring mass systems - to control the displacements at the deck level under seismic and ice loads for an offshore jacket structure. Jacket is a fixed structure and seismic loads can cause it to vibrate in the horizontal directions. These motions can disintegrate the structure and lead to potential failures causing extensive damage including environmental hazards and risking the lives of workers on the jacket. Hence, it is important to control the motion of jacket because of earthquake and ice loads. We analyze an offshore jacket platform with a tuned mass damper under the earthquake and ice loads and explore different locations to place the TMD. Through, selected parametric variations a suitable location for the placement of TMD for the jacket structure is arrived and this implies the design applicability of the present research. The ANSYS*™ mechanical APDL software has been used for the numerical modeling and analysis of the jacket structure. The dynamic response is obtained under dynamic seismic and ice loadings, and the model is attached with a TMD. Parameters of the TMD are studied based on the 'Principle of Absorption (PoA)' to reduce the displacement of the deck level in the jacket structure. Finally, in our results, the proper mass ratio and damping ratios are obtained for various earthquake and ice loads.

Keywords: anti-vibration device; parametric study; vibration control effect; seismic time history; dynamic ice force

1. Introduction

The 'Tuned Mass Dampers (TMDs)' are a class of the anti-vibration devices that are used to control the vibration under dynamic loads, e.g., seismic load, wave load, ice load and wind load, etc. In offshore structures, it can be used in both types of platforms, i.e., fixed and floating structures. The TMDs are used to mitigate vibration in the structure so that it is less susceptible to dynamic loads (e.g., Seismic, wave, ice and wind loads or a combination of them). In the case of offshore structures, a TMD system can be placed at the top of deck to maximize its effect. Theoretically, a TMD can be any one or a combination of: spring mass systems, tanks of water,

∗Corresponding author, E-mail: rajivatri@iitm.ac.in
[a] E-mail: rhtshrm95@gmail.com
[b] E-mail: v.domala@snu.ac.kr

and pendulum, etc. In the larger context of civil engineering, engineers have demonstrated the value of TMDs in experiments with real buildings, e.g., the researchers found that when a six storied building is subjected to earthquake-like vibrations, the TMD reduces the amplitude of the buildings oscillations by around 56%. Herein, we show that a TMD can be effectively used on a fixed offshore structure. Our results are numerical and are reported using ANSYS^{*TM} mechanical APD (2013).

The concept of TMD was applied by Frahm (1909) to reduce the rolling motion of ships as well as ship hull vibrations. A detailed description was presented later by Hartog (1947). Kawano *et al*. (1992) showed the analysis for a jacket structure of 120 m height subjected to two types of earthquake loads, ELCENTRO (1940) and TAFT (1962). Yue and Bi (2000) presented an analysis of an offshore structure subjected to acceleration of deck caused by drifting ice sheets in the Bohai Sea. Their study showed that the natural frequency of narrow or flexible structures is close to cyclic ice force and it can cause excessive vibration in the structure. Patil and Jhangid (2005) discussed the use of visco-elastic dampers and friction dampers and these can be used at every level of the structure to reduce the vibration caused by wave forces. Ou *et al*. (2007) placed a rubber isolator between the deck and jacket of a scaled model of JZ20-2MUQ platform and considered a simplified model (i.e., 6 degrees of freedom system) and presented analysis with SACS^{**TM} software to show the reduction of vibration under earthquake and ice loads. Yue *et al*. (2009) presented a design of the 'Tuned Mass Damper (TMD)' whose aim is to control the horizontal vibration under ice loads. Ma *et al.* (2010) discussed a detailed model study on jacket that was built in ANSYS^{*TM} using pipe elements and their analysis was performed under dynamic loads. Their results showed that the displacement at deck level reduces with the use of a TMD.

Recently, Zhang and Han (2014) developed a network based active control of jacket platform using a tuned mass damper. Motivated by them, several 'Network Based State Feedback Controllers (NBSFCs)' have developed to control the motions of the jackets and the researchers studied the reduction in motion with and without NBSFCs and observed that the NBSFCs reduced the motions of the jacket. Haeri *et al.* (2017) studied the health monitoring of the jacket platform using an inverse vibration technique using different models: 2D shear model, 2D flexural model and 3D shear building model. In their simulations the induced damages are applied to the members of jacket and their result showed that the 2D shear model was able to find the level of damage but not the extent of damage, it is not predicted accurately; 2D flexural model can predict the level of damage and extent of damage; and 3D shear model can locate the damaged member. Huang *et al.* (2017) reported an experimental study on ice pile up problem for a jacket platform for different ice velocities and ice angle attack. This study was conducted in the towing tank for different water levels and their results showed that for a high water level the upward bending failure of ice on jacket front can accelerate the water ice accumulation in the conductor array and for the lower water level the downward bending failure of ice on jacket front can help the underwater accumulation of ice rubble in the conductor array. Som and Das (2018) developed a semi active control algorithm using the 'Magneto-Rheological (MR)' damper and they considered seven cases by placing the MR damper at different locations on the jacket platform. Their results showed that placing the MR damper at different locations can result into the vibration control of jacket. Again, Hokmabady *et al.* (2019) studied the vibration of jacket using the MR tuned liquid column gas damper with varying gas pressure and yield stress and their results showed that this MR tuned liquid column gas damper can reduce the response by a larger percentage in comparison with the tuned liquid column gas damper without the MR.

Based upon the above observations, we state the objectives of the present work:

- (A) We analyze TMD systems without damping. This leads to several interesting observations that are helpful in designing the TMD. For these systems we primarily use a spring mass system as a TMD.

- (B) Unfortunately, when we analyze a structure with damping on both the structure and TMD, we cannot obtain the solution analytically and here we settle for numerical solutions. In the numerical model, we use two MASS21 elements and two COMBIN14 elements from ANSYS*TM.

A jacket structure of 74 m height is modeled in ANSYS*TM using PIPE16 and PIPE59 elements. This jacket structure is analyzed with two types of earthquake loads, i.e., ELCENTRO (1940) and KOBE (1995). The load is applied in the form of time acceleration series at the fixed end of structure and the TMD is attached at its top to reduce the deck displacement. After earthquake loads, the jacket is also analyzed under ice load in the form of ice force time series at jacket leg nodes along the water line and a TMD is designed for the same. This paper follows the basic ideas of our earlier work (Sharma *et al.* 2014) and now we present a detailed study of an anti-vibration device for jacket structure. However, some of the implementation details have been given only briefly here to keep the paper of reasonable length. A comprehensive treatment of all the examples with full theoretical and implementation details can be found in Sharma (2014).

2. Numerical formulations

2.1 Concept of the TMD

A large structure can be modeled as a single or combination of multiple simple spring mass systems. Whenever waves or any dynamic load hit the offshore structure, it applies a force on the structure. A structure if it is fixed or gravity supported does not move much because the steel legs and bays on each of sides are either rigidly connected or weight (gravity) supported to account for a small deformation only and restrict any large deviation. They create a push back effect against the load with a restorative force. This implies that the frame of a structure can be conceived to behave similar to a spring. We build upon this conception and we consider a spring mass system with three primary elements: a spring, a mass, and a damper. And, this system can be used to model a structure as shown in Fig. 1(a). In Fig. 1, the M is the mass of the structure, $F(t)$ is a force function of frequency ω (rad/s) that represents the wave, earthquake, wind or other external force applied to the structure, K (N/m) is the spring constant of the structure which is called stiffness, and C (N s/m) is its damping constant which represents the structure's resistance to movement.

Now, following Wilson *et al.* (2002), the model's mass' behavior is

$$M\ddot{x} + C\dot{x} + Kx = F\cos(\omega t) = F(t) \tag{1}$$

and Eq. (1) can be solved using steady state method used by Hartog (1947) and the solution yields a displacement function ($x_1(t)$), that describes how far the mass is from its equilibrium position at an instant of time (t), i.e.

$$x = x_1 + x_2 \tag{2}$$

$$x_1 = C_1 e^{-\omega \xi t} \cos(\omega_d t - \theta) = C_1 e^{-at} \cos(\omega_d t - \theta) \tag{3}$$

$$x_2 = B_1 \sin \omega t + B_2 \cos \omega t \tag{4}$$

where x_1 is the complementary function, x_2 = particular integral, C_1, B_1, B_2 are integral constants, ω is the frequency in rad/s, ω_d is damping frequency and ξ is the damping ratio. The complete solution of Eq. (1) with conditions of Eqs. (2)-(4) is

$$x = C_1 e^{-at} \cos(\omega_d t - \theta) + \frac{F}{\sqrt{C^2 \omega^2 + (K - M \omega^2)}} \times \cos(\omega t - \varphi) \tag{5}$$

where θ is phase angle and φ is $\tan^{-1}\left(\dfrac{C \omega}{(K - M \omega^2)}\right)$, and other terms are as defined previously. The frequency, at which the amplitude is maximum, is the resonant frequency and it is the natural frequency of the structure (Ω). In the case of without damping the Ω is

$$\Omega = \omega_n = \sqrt{\frac{K}{M}} \tag{6}$$

2.2 A brief demonstration of Hartog's (1947) technique

A basic spring mass system attached with the TMD is shown in Fig. 1(b). In Eq. (1), we assume that there is no damping and then taking the free body diagram for both the masses we get

$$M \ddot{x}_1 = - K x_1 - k (x_1 - x_2) + F_0 \sin \omega t \tag{7}$$

$$m \ddot{x}_2 = - k (x_2 - x_1) \tag{8}$$

where M is the primary mass, m is the secondary mass, K is the stiffness of primary mass, k is the stiffness of secondary mass, ω is the frequency of the forcing function (F_0), x_1 is the displacement of primary mass, and x_2 is the displacement of secondary mass. Let $x_1 = A \sin \omega t$ and $x_2 = B \sin \omega t$, and substituting them in Eqs. (7) and (8) we get:

$$M(-\omega^2 A \sin \omega t) + (K + k) A \sin \omega t - k B \sin \omega t = F_0 \sin \omega t - k A \sin \omega t + (k - m \omega^2) B = 0 \tag{9}$$

and then dividing by $\sin \omega t$ we get

$$B = \frac{k A}{k - m \omega^2}, \text{ and } A = \frac{F_0 (k - m \omega^2)}{[(K + k - M \omega^2)(k - m \omega^2) - k^2]}. \tag{10}$$

Therefore

$$x_1 = \frac{F_0(k - m\omega^2)}{\{(K + k - M\omega^2)(k - m\omega^2) - k^2\}} \sin \omega t \tag{11}$$

$$x_2 = \frac{F_0 k}{\{(K + k - M\omega^2)(k - m\omega^2) - k^2\}} \sin \omega t \tag{12}$$

Using Eqs. (11) and (12) the response of a structure can be found under harmonic load if all the parameters are known. The response to harmonic exciting force is harmonic because of the $\sin \omega t$ term present in the solution. The above equation only represents the steady response and the transient portion is neglected because of the exponential term. To compare the numerical results of ANSYS[*TM] (2013) with the analytical results of Equations given above, we consider a single primary mass and mass ratio of 0.1 for the secondary mass and using the analytical solutions of Hartog's (1947), we get:

$$f = \frac{1}{1 + \mu} \quad \text{and} \quad \xi = \sqrt{\frac{3\mu}{8(1 + \mu)^3}}$$

where f is the tuning factor, ξ is the damping ratio and μ is the mass ratio. We assume $M = 10$ kg, $m = 1$ kg, $C = 1.2$ N/m/s, $c = 0.3$ N/m/s, $K = 90$ N/m, and $k = 9$ N/m. Then, using Equations (4 and 5), we get the response of primary mass with and without TMD and it is shown in Fig. 2. A jacket structure is built in ANSYS[*TM] (2013) and a forcing function of $F\cos(\omega t)$ is used to excite the structure along 'y' direction. The responses are computed for two conditions (i.e., with and without TMD) and shown in Figs. 2(a) to 2(d). Figs. 2(a) and 2(c) show the computed response using ANSYS[*TM] and Figs. 2(b) and 2(d) show the computed response using Equations (4 and 5). The analytical static solution is computed and compared with the ANSYS[*TM] (2013) results. The response of offshore structure (i.e., jacket) at $\mu = 0.1$ is found to be 4.3 mm and 4.05 mm respectively between the analytical and numerical results. Our results show that in between the analytical and numerical results there is a small error of around 6%, i.e., error = ((4.30-4.05)/4.30)*100 = 5.814 %. This error happens mainly because of the approximation of mass matrix in the analytical and numerical approaches and this error will remain.
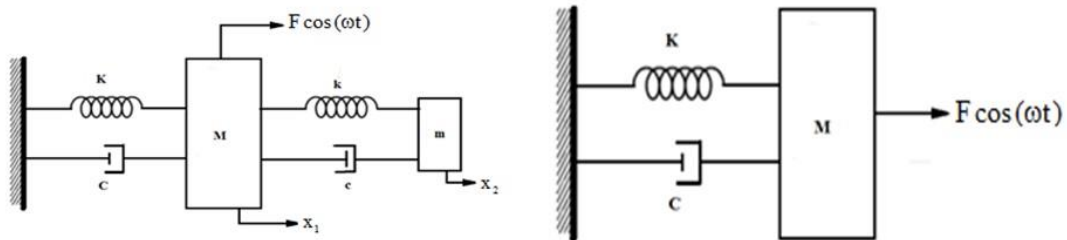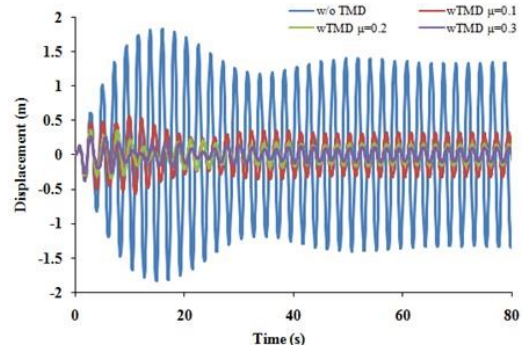

(a) Schematic of the basic spring mass system   (b) A basic spring mass system attached with TMD
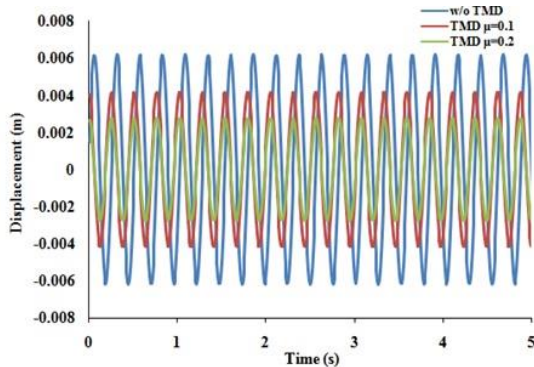
Fig. 1 Schematic of the basic spring mass system and its attachment with the TMD
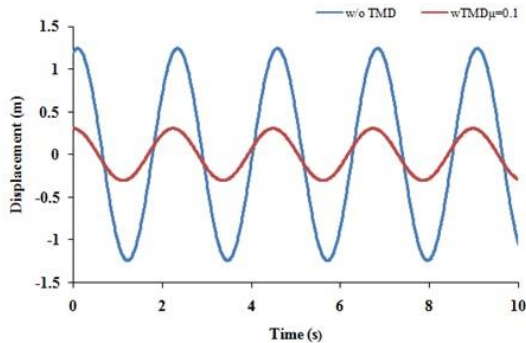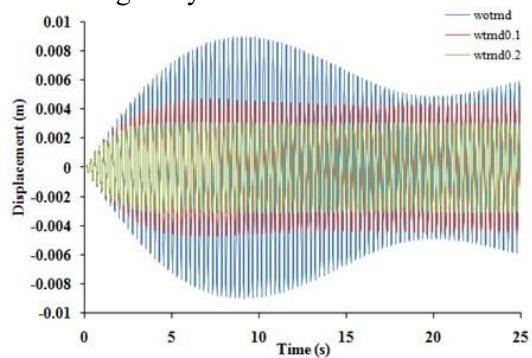
(a) Computed displacement of primary mass using ANSYS*TM

(b) Computed displacement of the primary mass using analytical solution

(c) Computed response at the deck level using ANSYS*TM mechanical APDL

(d) Computed response under the harmonic load using analytical solution

Fig. 2 Computed displacement of the primary mass and response at the deck level of offshore structure

However, the error is small and it shows that the results are in close agreement for all the practical applications. Although, in the present paper for detailed results and discussion, we focus primarily at the $\mu = 0.1$, we have considered other values of the μ (i.e., 0.2, 0.3, etc.) and some results corresponding to them are shown without discussion as they follow the same trend.

3. Tuned mass damper concept for SDOF

3.1 Un-damped TMDs

In reference to Fig. 1(b), we assume that the $C = c = 0$, and it implies that there is no damping in the TMD. Since, adding a TMD changes the natural frequency of the system, so instead of having one natural frequency for the system (Ω), we have two, i.e., natural frequencies ω_1 and ω_2. Time acceleration series of the ELCENTRO earthquake of 1940 adapted from PEER (2007) is shown in Fig. 3(a). In Fig. 3(b), we show these two natural frequencies as the peaks in graph. We
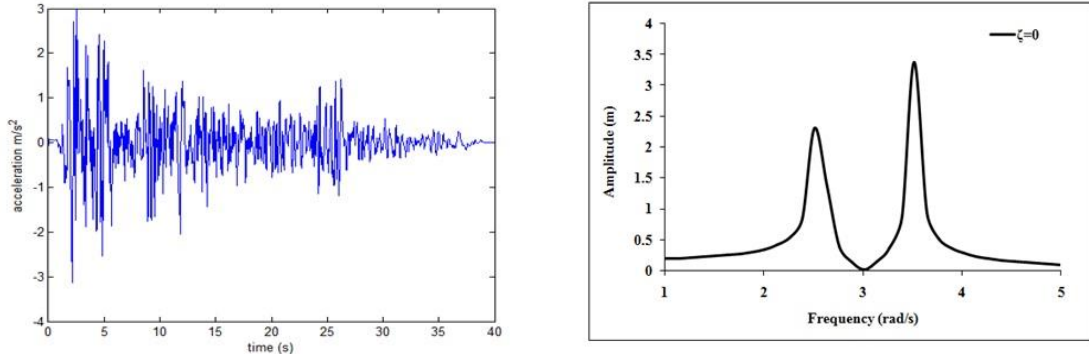
(a) Time acceleration series of ELCENTRO earthquake of 1940

(b) Computed response amplitude as a function of the driving frequency (ω)

Fig. 3 Computed response amplitude as a function of the driving frequency (ω) and time acceleration series of ELCENTRO earthquake of 1940 adapted from PEER (2007)

note here that Fig. 3(a) is a time series and Fig. 3(b) is the amplitude response of time series given in frequency domain. Now, when the denominator of a steady state solution of $x_1(t)$ is either equal or approaching to zero, then we have resonance and the $x_1(t)$ has an infinite amplitude in its oscillation. Thus, the closed form solution of ω_1 and ω_2 is

$$\omega_1 = \frac{\sqrt{\dfrac{-\sqrt{(kM-Km)^2+2k^2Mm+2Kkm^2+k^2m^2}}{mM}+\dfrac{K}{M}+\dfrac{k}{M}+\dfrac{k}{m}}}{\sqrt{2}} \text{ , and} \tag{13}$$

$$\omega_2 = \frac{\sqrt{\dfrac{\sqrt{(kM-Km)^2+2k^2Mm+2Kkm^2+k^2m^2}}{mM}+\dfrac{K}{M}+\dfrac{k}{M}+\dfrac{k}{m}}}{\sqrt{2}} \tag{14}$$

where all the terms are as defined previously. This results of Eqs. (13) and (14) are interesting because the ω_1 and ω_2 differ only in sign of one term and although the computed frequencies appear to be symmetric about $\dfrac{\sqrt{\dfrac{K}{M}+\dfrac{k}{M}+\dfrac{k}{m}}}{\sqrt{2}}$, they are not exactly symmetric because we take the square root of the entire expression.

3.2 Definition of the optimization based approach

Although, we can assume $C = c = 0$, it is difficult to define because always there exist some resonant frequencies that can cause extremely large (i.e., infinite) response amplitudes. We assume that the values for spring constant (K) and the mass (M) are given by the nature of structure. In this case of single TMD with no damping, we define the optimal in two ways: 1) we minimize the amplitude of primary mass at its original natural frequency, and 2) we maximize the separation between original natural frequency of the structure (Ω) and the nearest peak frequency (ω_1 or ω_2). We observe that the vibration is minimized when the TMD system has the same natural frequency as the single mass system. This causes the amplitude of structure's vibration to be almost zero when excited at Ω. In the second approach, we maximize $[\min(|\Omega - \omega_1|, |\Omega - \omega_2|)]$. This means that any frequency around the original natural frequency of building is not expected to produce any dangerously high levels of vibrations. This is expected to create as large a safety interval as possible around Ω and it will make the structure less vulnerable to the susceptibility from periodic forces (e.g., earthquake force).

3.3 Optimizing un-damped TMDs

In the second approach, we observe that as the mass of the damper (m) increases, the distance between Ω and ω_1 or ω_2 grows. So, to optimize we can simply make (m) infinitely large. However, that is impractical. Thus, we assume that a maximum value is given for (m) by the engineers. Since, a high value of the m is always advantageous, we use the high value of m and after selection of m the only remaining parameter that needs to be adjusted is the spring constant (k) of the TMD.

4. Jacket modeling and analysis

4.1 Jacket modeling

The idea of anti-vibration device of this paper is implemented on a jacket platform. The numerical modeling for the jacket is done in ANSYS[*TM] (2013) using the 'ANSYS Parametric Design Language (APDL)'. A node is created at each of the joints by specifying (x, y, z) coordinates and then these nodes are joined using a line command. These lines are meshed and elements are created. Legs of jacket are assigned with 'PIPE 59' elemental properties in which pipe diameter, wall thickness, added mass per unit length and material properties such as Poisson's ratio and Young's modulus are given. The jacket braces are formed using 'PIPE 16' element and X-bracings are used too. The primary aim is to reduce the response of offshore structure at the deck level and the dynamic loads (i.e., earthquake and ice time acceleration series) are applied to check the response and performance of the TMD. The TMD is modeled using two elements from ANSYS[*TM] (2013): 'MASS 21' and 'COMBIN 14' elements. In the 'MASS 21' element a mass value can be given in any of the x, y, z directions. It is shown as a point in the 'Graphical User
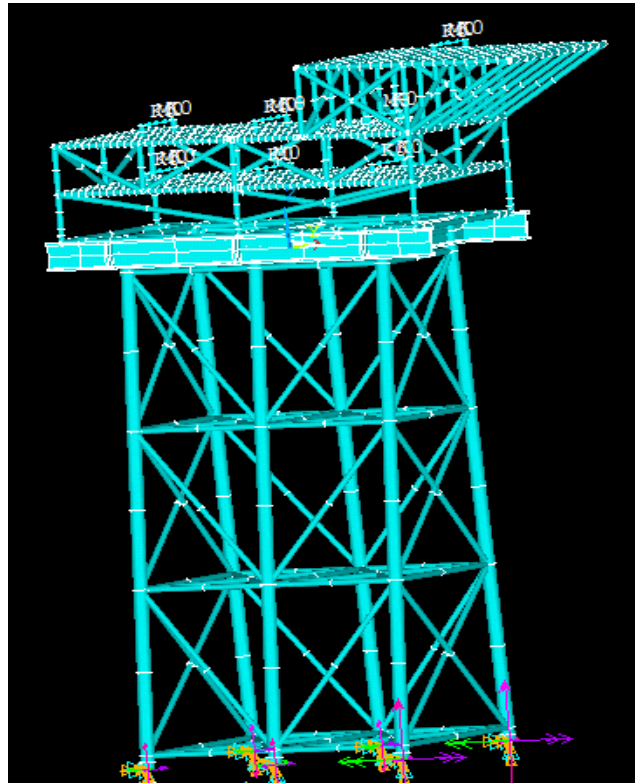
Fig. 4 Jacket modeled in ANSYS*TM (2013) mechanical (APDL)

Interface (GUI)' of ANSYS*TM (2013). The 'COMBIN 14' element acts as a spring and damper and in this stiffness and damping values can be entered numerically. The jacket model in ANSYS*TM (2013) mechanical (APDL) is shown in Fig. 4. The total number of PIPE 59 elements is 138 and the jacket specifications are: jacket height = 74 m, deck levels are two (lower deck +10 m and upper deck +17 m). Detailed jacket specifications are listed in Table 1. Dynamic loads are applied in the horizontal direction, e.g., '*y*' direction.

Table 1 Specification of jacket structure

Jacket leg element	Pipe 59
Total pipe 59 elements	138
Jacket height (m)	74
Jacket leg diameter (m)	2
Wall thickness (m)	0.03
Bracing element	Pipe 16
Bracing diameter (m)	0.85
Bracing wall thickness (m)	0.025
Mass of structure (MT)	7123.5
Poisson' ratio	0.3
Young/s modulus (N/m^2)	2×10^{11}

Table 2 Computed natural frequencies for different modes

Mode	1st	2nd	3rd	4th
Frequency (Hz)	0.33143	0.38532	0.45603	0.56106

4.2 Modal analysis

In ANSYS[*TM] the jacket structure is fixed at its bottom by constraining all the 'Degrees of Freedom (DoFs)' at the bottom nodes and under no load condition modal analysis is performed to find the natural frequency of the structure. The mode extraction method used in ANSYS[*TM] (2013) is the 'Block Lanczos Method (BLM)' and it is an efficient method to perform a modal analysis for the large models of offshore structure. The computed natural frequencies for different modes are listed in Table 2.

4.3 Harmonic analysis

The harmonic analysis is performed to compute frequency responses and through the frequency response the dominant frequency of the structure is arrived at, i.e., by observing the peak. In the harmonic analysis a load is assigned to the structure, and it can be either static or dynamic. The three solution methods are available: 1) reduced, 2) mode superposition and 3) full solution. We use the full solution to observe the most dominant frequency.

4.4 Transient analysis

The transient analysis is a time varying analysis, and in it a time varying load is assigned to the structure. Then the responses are found at each of the time steps. The acceleration data of earthquake load is given to the fixed nodes at the bottom in the form of ground acceleration and the displacement at deck level nodes is noted down with and without the TMD.

The transient dynamic analysis is used to determine the time history dynamic response of a structure to arbitrary forces varying with time. This analysis yields the displacement, strain, stress and force time history responses of a structure to any combination of transient or harmonic loads. To obtain the solution of the equation of motion (1) a time integration method is employed. There exist two types of methods: Implicit and explicit methods.

Normally, the implicit method is unconditionally stable and that implies that various time step sizes can be chosen without any limitations. Because of this we use implicit method in this paper.

4.5 Implicit time integration and its application

We use the implicit time integration (Newmark's method 1959) and implement it through an inbuilt algorithm in ANSYS[*TM] (2013). The stability of method is controlled by two parameters that are set up by default so that the scheme is unconditionally stable and the effect of numerical damping is minimized. The application of the Newmark method (1959) to the equation of motion (1) results into a linear system of equation for each of the time steps. Since, the stiffness matrix appears on the left hand side, it needs to be inverted in each of the time steps in the incremental

solution process. Since, the inversion is a computationally expensive process more so for highly nonlinear problems, the implicit solution techniques offer an efficient choice to solve transient analysis problems if the problem is not crucially dominated by the nonlinearities. We use the Newmark's (1959) beta technique to compute the solution of multiple degrees of freedom (MDoFs) system subjected to a dynamic seismic load.

4.6 Seismic analysis in ANSYS^{*TM}

The time acceleration series of earthquake is applied to the fixed base and responses are collected using the transient analysis. The transient analysis is used to perform time varying dynamic analysis. As the seismic load is time varying it is given to the structure using 'ACEL command' in ANSYS^{*TM} APDL (2013).

To implement, in ANSYS^{*TM} APDL (2013), we first create a table which carries the seismic loads in the form of time acceleration series and then the seismic load text file is named and called in the ANSYS^{*TM} APDL (2013) program using '*GET' command. Then, using the DO loop seismic load is applied to the structure base at every step of 0.01 s, and this is a time consuming process because of large load time and smaller time periods. Now, the displacement, velocity, acceleration, and stress, etc., are computed at every node.

4.7 Analysis under dynamic ice load

In cold regions, for example Bohai Sea, the ice sheets are formed over the water layer and their thickness can vary from 0.1 to 0.8 m. Also, they drift with a velocity of 10 cm/s to 60 cm/s. The frequency of these ice forces varies from 0.1 Hz to 1 Hz, and because of this when they hit narrow structures in the ocean such as the jacket legs, there is a chance of structure coming into resonance with the forcing function.
Following, Yue and Bi (2000) the forces on the narrow structure in cold regions are

$$F(t) = \begin{cases} F_0(1 - \dfrac{t}{\tau}) , & 0 \le t < \tau \\ 0 & , & \tau \le t < T \end{cases} , \text{ and} \tag{15}$$

$$T = \frac{L}{V} \tag{16}$$

$$L = 7.3h \tag{17}$$

where F_0 is the maximum global ice force (N), τ is the time period which relates breaking length during ice slab rotating, V is the drift velocity of ice sheet (m/s), T is the time period between two consecutive ice breaking (s), L is the length of the broken ice piece and h is the height of the broken ice piece.

To study the effect of TMD on controlling these vibrations, a jacket (JZ20-2) is modeled in the ANSYS^{*TM} (2013) and the time acceleration series of the data belonging to Bohai sea is considered as an input. This time acceleration series is applied at the nodes of jacket leg at the water level and the displacement is recorded at the deck level for the various mass ratios and TMD parameters. The acceleration time history of the deck of JZ20-2 is shown in Fig. 5.
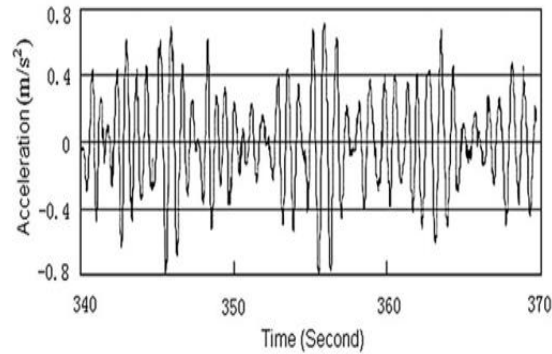
Fig. 5 Acceleration time history of the deck of JZ20-2 operating at the Bohai Sea, adapted from Yue *et al*. (2009)

5. Results and discussions

5.1 Jacket under Elcentro seismic load

The load via time acceleration is applied to the structure base in ' *y* ' direction and a transient analysis is performed. The time acceleration series of ELCENTRO earthquake of 1940 adapted from PEER (2007) is used and has already been shown in Fig. 3(a).

5.2 Testing TMD at different positions

We explore the different TMD positions and overall 7 TMDs are installed at the various locations. Even though 7 TMDs are used, all of them are not used at once and only one TMD is tested at different locations on the jacket with different mass ratios. A mass ratio of 0.065 is taken and the reduction in responses due to each of the TMDs individually is compared. The other technical details are: TMD1: at a height of 27 m from the water level and 25 m away from the CoG horizontally; TMD 2 and TMD 4: at a height of 17 m from the water level and 15 m away from the CoG horizontally; TMD 3: above CoG, on upper deck; TMD 5 and TMD 7: at a height of 10 m from the water level and 15 m away from the CoG horizontally; and TMD 6: vertically above the CoG, on the lower deck. The various TMD positions on deck are shown in Fig. 6 and TMD positions are listed in Table 3. In the present study, only one TMD has been tested at different positions along with different mass ratios. All the TMDs have not been used at once because using all the TMDs at once will increase the mass of the structure significantly and that is neither desirable nor feasible nor economical. Hence, only one TMD has been tested at each of the positions.

5.3 Response at various mass ratios

The TMD 6 shows a better performance (Sharma 2014), and because of this its mass ratio is changed and the effects are studied in detail. These results are shown in Fig. 7. Fig. 7(a) shows the

response of deck level with the different TMDs functioning at various locations with the same m, c, and k values. We see from the results that the TMD 6 offers a higher reduction in the displacement of deck compared to the other TMDs. The position of TMD 6 is above the CoG of structure and this implies that an effective TMD needs to be vertically in-line with the CoG of structure and the distance needs to be as close as possible from fabrication point of view.

Additionally, from Fig. 7(b) we observe that a larger reduction in the responses is possible in the range of $\mu = 0.06$ to $\mu = 0.09$, e.g., the reduction in displacement is 57.14%. At the lower values of μ (e.g., 0.025), the reduction in response is very less and it implies that the TMD at lower mass ratios are not able to offer any significant resisting force to the exciting dynamic force. A medium ratio of μ (e.g., 0.05) shows better reduction in the response and similarly a higher ratio of μ (e.g., 0.06) shows a reduction of 52%.
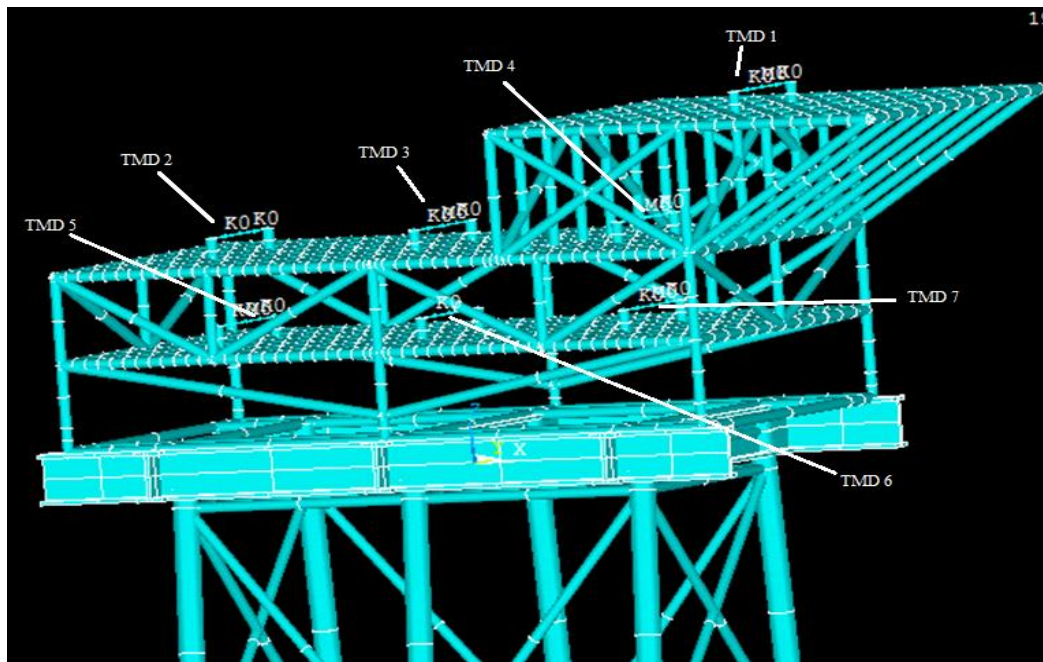

Fig. 6 Various TMD positions on the deck

Table 3 Details of the positions of TMDs on jacket platform

	Positions of TMDs on jacket platform
TMD 1	27 m above the sea level and 25 m away from the CoG
TMD 2 and 4	17 m above the sea level and 15 m away from the CoG horizontally
TMD 3	Above the CoG on upper Deck
TMD 5 and 7	10 m above the sea level and 15 m away from the CoG horizontally
TMD 6	Vertically above the CoG

5.4 TMD on upper deck with different mass ratios

We observe that with the TMD 4, a similar reduction in the response is occurring at the higher mass ratios too because of the distance from the CoG. Instead of the $\mu = 0.063$, the TMD 4 takes up $\mu = 0.083$ to reduce the response by 58%. This is shown in Fig. 8(a). Table 4 shows the displacement of the deck of offshore platform. Figs. 8(b) shows the comparison of displacement of jacket deck level with and without TMD at $\mu = 0.063$ and $\mu = 0.083$. Fig. 9(a) shows that a TMD is effective when the μ varies from 0.06 to 0.12. Fig. 9(b) shows that a favorable frequency ratio is in between 0.83 to 0.93.

5.5 Finding the area required for TMD

In the process of optimizing TMD parameters, we compute the mass and stiffness of the structure. Using these parameters of the mass and stiffness, we compute the required area of TMD on the deck of platform. As the mass is known and using the steel material (i.e., known density) we compute the required volume. Then, we design the spring mass system using concepts from Wahl (1944) and following it the diameter of wire is

$$d \geq 1.6 \sqrt{\frac{F_{s\max} CK}{\sigma_\tau}} \tag{18}$$

The number of coils is given by

$$n = \frac{Gd^4}{8D^3 k} \tag{19}$$

where G is the shear modulus of material (0.8×10^{11} N/m^2), C is the spring index (assumed 10), σ_τ is the permissible shear stress of material (325×10^6 N/m^2), k is the stiffness of each of the springs (kN/m), $F_{s\max}$ is the maximum load on each of the springs in N, n is the number of coils, d is the diameter of spring wire, $D = (2r)$ is the mean spring diameter, and K is the stress correction factor and it is

$$K = \frac{4C-1}{4C-4} + \frac{0.615}{C} \tag{20}$$

The stress correction factor for helical springs is shown in Fig. 10. The TMD is designed for the mass ratio $\mu = 0.063$ and the other parameters are:

  Total mass of jacket = 7123.5 tones,
  Mass of TMD = 448.78 tones,
  Using steel as the material having density of 7.860 ton/m^3,
  Weight of a cuboid of $3.8 \times 3.8 \times 3.8$ m = 448.78 tones, and
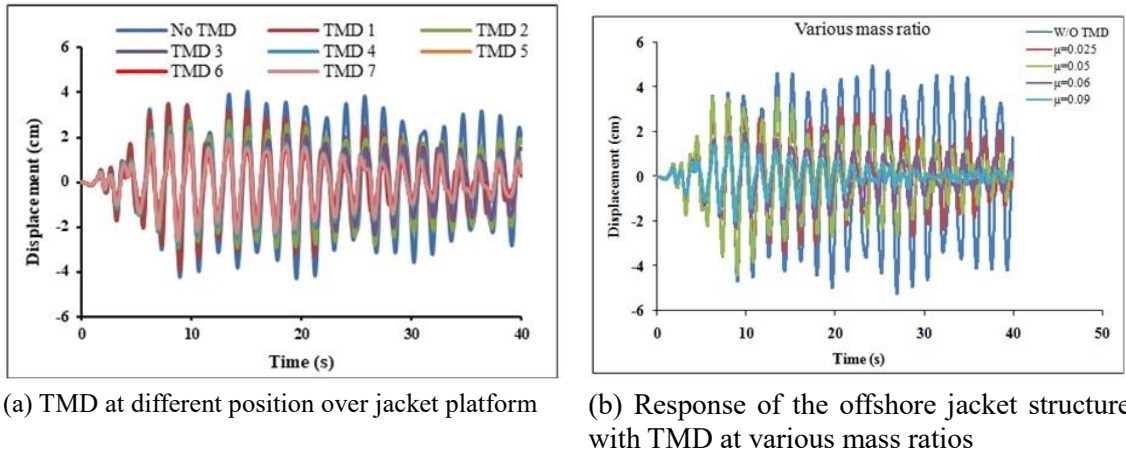 $k = \omega^2 m$, 557.637 kN/m.

(a) TMD at different position over jacket platform

(b) Response of the offshore jacket structure with TMD at various mass ratios

Fig. 7 Effect of position of TMD and response at various mass ratios

(a) Response reduction of the offshore jacket structure with TMD 4

(b) Response reduction of the offshore jacket structure with TMD at μ=0.063 and μ=0.083
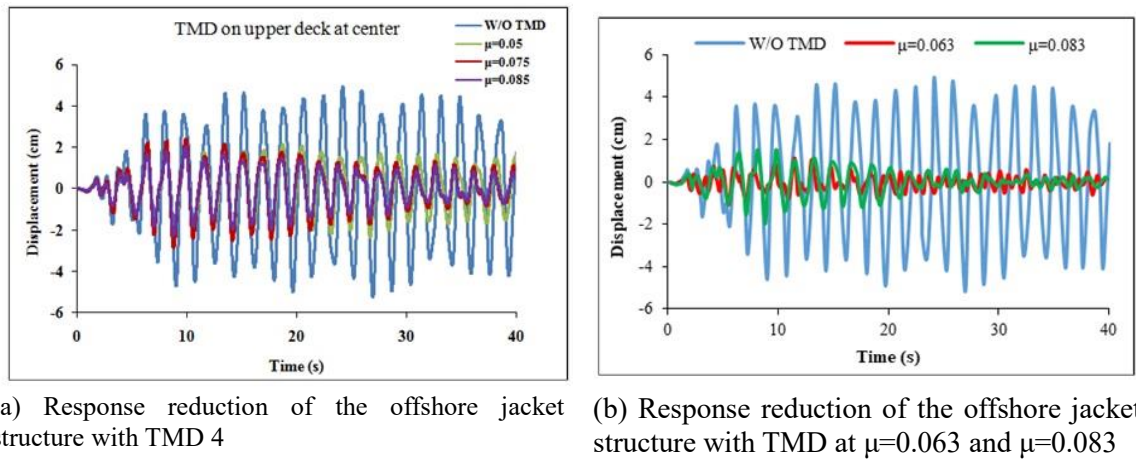
Fig. 8 Comparison of response reduction between with and without TMD, and with TMD 4 and 6

Using 8 springs - 4 on each of the sides - we arrive at the stiffness of spring as 69.70 kN/m, acceleration of TMD mass is 4.3 m/s² and the maximum force on each of the springs is:

$$F_{smax} = \frac{44878 \times 4.3}{4} = 48.243 \text{ kN.}$$

Using Eqs. (18) and (19), we arrive at: $d \approx 0.066 = 0.07$, $D = 700 \ mm$, and $n \approx 10$ coils.

The lengths of spring are:

Solid length (L_s) = $(n+2)d = 0.84$ m,

Free length (L_f) = $L_s + \Delta \approx 1.6$ m,

where Δ is the maximum deflection. Now, the approximate area required for the TMD is: $(3.8+1.6)^2 = 30 \text{ m}^2$, and this is around 2% of the total deck area.

5.6 Jacket under Kobe (1995) earthquake load

The KOBE earthquake time acceleration is shown in Fig. 11(a). And, the computed response under KOBE (1995) for various mass ratios is shown in Fig. 11(b). From Fig. 12(b), we can see that under KOBE (1995) earthquake load the maximum reduction is happening at $\mu = 0.083$. However, compared to the mass ratio of $\mu = 0.063$, the reduction is almost same.
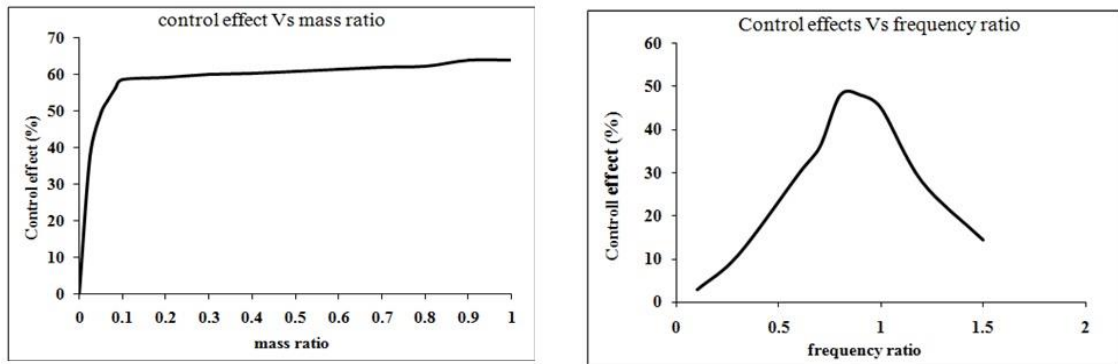
(a) Computed response of the control effect by changing mass ratio

(b) Computed response of the control effect by changing frequency ratio

Fig. 9 Computed control effect by changing the mass ratios and frequency ratios
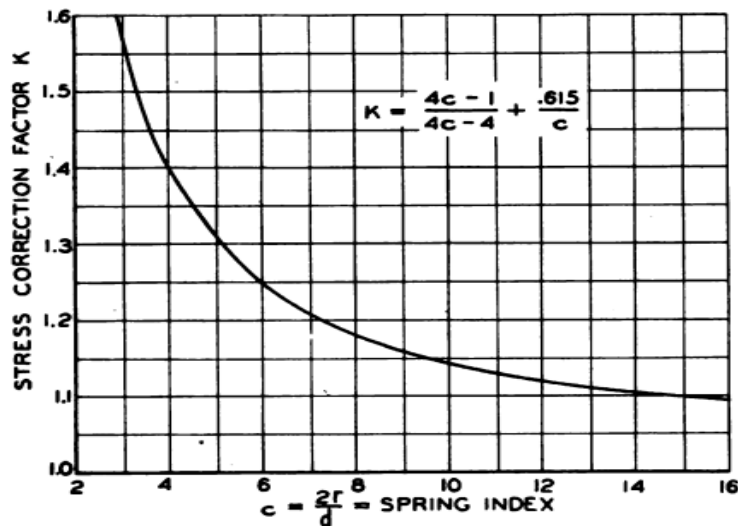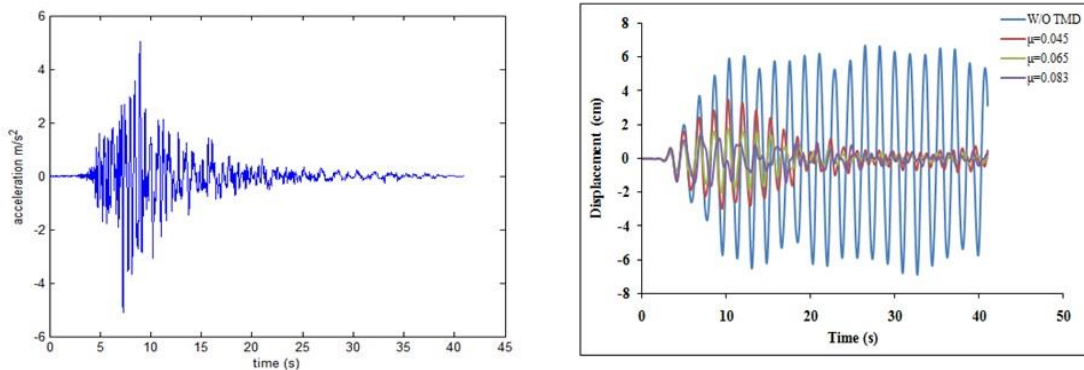

Fig. 10 Stress correction factors for the helical spring, adapted from Wahl (1944)

Table 4 Computed displacement of the deck platform at $\mu = 0.063$

Data record node number	Displacement with-out (w/o) the TMD (cm)	Displacement with the TMD (cm)	Vibration control effect (%)
762	4.33	1.95	54.96
767	4.31	1.92	55.45
772	4.39	1.87	57.40
776	4.34	1.83	57.83
783	4.39	1.76	59.90
788	4.25	1.70	60.00
791	4.22	1.81	57.10
797	4.19	1.86	55.60
801	4.28	1.88	56.10
808	4.32	1.92	55.55
Average			56.98

(a) Time acceleration series for KOBE (1995) earthquake adapted from PEER (2007)

(b) Computed response of the offshore jacket structure under KOBE (1995) for various mass ratios

Fig. 11 KOBE (1995) earthquake time acceleration series and the computed response for various mass ratios

Hence, it is better to use mass ratio of $\mu = 0.063$ to avoid increase in load over the platform. Tables 5 and 6 show the values of deck level displacements at various nodes with and without the TMD. The average reduction in computed response is 45.2% for the $\mu = 0.083$ and when the mass ratio is $\mu = 0.063$, then the reduction in computed response is around 54.42%.

Table 5 Computed displacement of lower deck with μ=0.083

Data record node number	Displacement w/o the TMD (cm)	Displacement with the TMD (cm)	Vibration control effect (%)
762	6.20	3.31	46.61
767	6.23	3.56	42.85
772	6.15	3.48	43.41
776	6.28	3.26	48.08
783	6.18	3.52	43.04
788	6.05	3.28	45.78
791	6.22	3.35	46.14
797	5.98	3.24	45.82
801	6.31	3.44	45.48
808	6.11	3.38	44.68
Average			45.20

Table 6 Computed displacement of lower deck with μ=0.063

Data record node number	Displacement w/o the TMD (cm)	Displacement with the TMD (cm)	Vibration control effect (%)
762	6.20	2.81	54.67
767	6.23	2.76	55.69
772	6.15	2.98	51.54
776	6.28	2.76	56.05
783	6.18	2.62	57.60
788	6.05	2.88	52.39
791	6.22	2.85	54.18
797	5.98	2.64	55.85
801	6.31	2.94	53.40
808	6.11	2.88	52.86
Average			54.42

5.7 Analysis under dynamic ice load

In the cold regions, it is found that the ice in various forms deposits over the deck platform, e.g. snow fall. The thickness of ice deposits can vary from few mm to 0.5 m and even to 1 m thick in the rare cases. We consider the ice deposit of thickness of 0.3 m and density of 910 kg/m^3. The open deck area is 1500 m^2, and so the total weight of ice is 410 tons. At $\mu = 0.063$, the reduction in the computed response is around 53.3%. And, this can be further reduced by increasing the mass ratio, e.g., at $\mu = 0.09$ the computed responses are listed in Table 7.

Table 7 Computed displacement of lower deck with μ=0.09

Data record node number	Displacement w/o the TMD (mm)	Displacement with the TMD (mm)	Vibration control effect (%)
762	5.8	2.43	58.10
767	5.82	2.52	56.70
772	5.75	2.45	57.39
776	5.72	2.28	60.13
783	5.81	2.39	58.86
788	5.68	2.45	56.87
791	5.85	2.41	58.80
797	5.77	2.35	59.27
801	5.7	2.3	59.64
808	5.65	2.32	58.93
Average			59.46
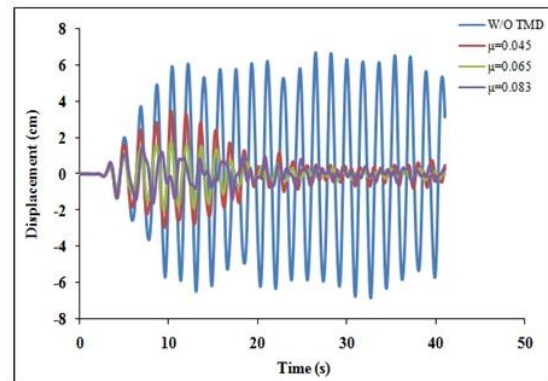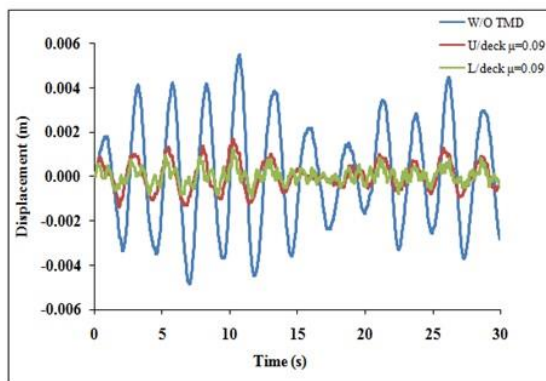
(a) Computed offshore platform deck response at μ=0.09

(b) Computed offshore platform deck response at μ=0.0851 with dead load of 410 tons

Fig. 12 Computed offshore platform responses with $\mu = 0.09$ and dead load of 410 tones for $\mu = 0.045$ to 0.083

We observe from the results of Table 7 and Figs. 12 and 13 that if the mass ratio is increased up to $\mu = 0.09$, then the response reduces further but it is not an efficient design choice to put an additional heavy mass on the structure. By adding a dead load of 410 tons over the deck and checking the response with the same mass ratio we obtain the results that are shown in Fig. 12(b). From Figs. 13(a) and 13(b), we can see that as the dead load increases the frequency of structure changes and that adversely affect the performance of the TMD. However, it can still remain effective because the changed frequency can still be in the frequency range of the TMD. If the mass ratio is more than the range of TMD is wider and the jacket response can be reduced with higher amount of ice deposits over the structure. But, as observed earlier the higher mass ratio is
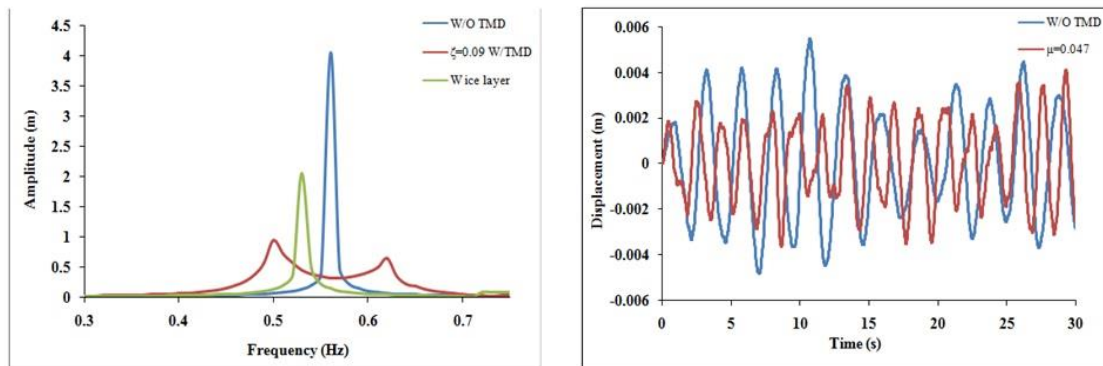
(a) Computed offshore platform deck response at μ=0.09

(b) Computed offshore platform deck response at μ=0.0851 with dead load of 410 tons

Fig. 13 Computed frequency response and response of the structure with increased dead load without/with TMD at $\mu = 0.047$

not feasible in any of the structures. Without the increase in deck load at $\mu = 0.05$ the TMD is 54 % effective but still we need to double the mass ratio so as to increase the range of TMD keeping in mind that the load on the structure can go up by 410 tones. As the total weight of structure reduces the mass ratio (μ) reduces from 0.05 to 0.047 and the new structure frequency (0.518 Hz) gets closer to one of the split frequency of the TMD (0.49 Hz). In this case the effectiveness of TMD reduces to 25.9% from 54%. Therefore, in the cases where there is possibility of increase or decrease in the dead load over the structure, the mass ratio should be kept little higher.

6. Conclusions

This paper presented an application of the TMD for an offshore structure (jacket) under two types of dynamic loads (i.e. seismic load and ice load). The parameters of TMD have been explored for various design choices. The major conclusions that can be drawn from this work are:
- With the TMD, at $\mu = 0.065$ the structure response is reduced to 58% under ELCENTRO (1940) load and under KOBE (1995) earthquake load the response reduces to 53%.
- The TMD needs to be vertically above CoG of structure and as close to it as possible.
- The TMD of size $(3.8m \times 3.8m \times 3.8m)$ is found using mechanical equations and it takes 2-3% of total deck area.
- The TMD is effective under the dynamic ice loads and mass ratio needs to be in between μ 0.047 to 0.090. With the increase of deck load due to ice deposition the TMD becomes less effective as the frequency of structure changes. And, it can become ineffective also if the frequency goes outside the TMD range.

Additionally, to ensure that the idea of present leads to an industrial application we need to focus on the detailed reliability analysis of the structure with TMDs and the cost benefit analysis, etc. Our future work shall go in these directions and some of them are currently under investigation.

Acknowledgements

Trademarks and copy rights

[*]Trademark and copyright with ANSYS Inc., USA. [**] Trademark and copyright with The Bentley Systems, USA.

References

ANSYS-Mechanical (APDL), (2013), 13.1, Ansys, Inc.- http://www.ansys.com/.

Frahm, H. (1909), "Device for Damping Vibrations of Bodies", US patent No.989958.

Haeri, H., Lotfi, A., Dolatshahi, K.M. and Golafshani, A.A. (2017), "Inverse vibration technique for structural health monitoring of offshore jacket platforms", *Appl. Ocean Res.*, **62**, 181-198.

Hartog, J.P.D. (1947), "Mechanical vibrations", McGraw-Hill publication, New York, N.Y.

Hokmadady, H., Mohammadyzadeh, S. and Mojtahedi, A. (2019), "Suppressing structural vibration of a jacket-type platform employing a novel magneto-rheological tuned liquid column gas damper (MR_TLCGD)", *Ocean Eng.*, **180**, 60-70.

Huang, Y., Sun, J., Wan, J. and Tian, T. (2017), "Experimental observation on the ice pile-up in the conductor array of a jacket platform in Bohai sea", *Ocean Eng.*, **140**, 334-351.

Kawano, K. and Venkatramana, K. (1992), "Seismic response of offshore platform with TMD", *Proceedings of the Earthquake Engineering Tenth Conference*, 179-188.

Ma, R., Zhang, H. and Zhao, D. (2010), "Study on the anti-vibration devices for a model jacket Platform", *Mar. Struct.*, **23**, 434-443.

Newmark, N.M. (1959), "A method of computation for structural dynamics", *J. Eng. Mech. Div. – ASCE*, **85**, No. EM3.

Ou, J., Lon, X., Lic, Q.S. and Xiao, Y.Q. (2007) "Vibration control of steel jacket offshore platform structures with damping isolation system", *Eng. Struct.*, **29**, 1525-1538.

Pacific Earthquake Engineering Research centre (PEER), (2007), www.peer.berkeley.edu.

Patil, K.C. and Jangid, R.S. (2005), "Passive control of offshore jacket platforms", *Ocean Eng.*, **32**, 1933-1949.

Sharma, R.K. (2014), "A study on anti-vibration device for a jacket structure", Master of Technology (M.Tech) Thesis, Department of Ocean Engineering, IIT Madras, India.

Sharma, R.K., Domala, V. and Sharma, R. (2014), "A research paper about a study of an anti-vibration device for jacket structure", *Proceedings of the Earthquake Engineering 15th Symposium on Earthquake Engineering (15 SEE – 2014)*, (Eds., Sharma, M.L. and Shrikhande M.), **1- 2**, 659-671.

Som, A. and Das, D. (2018), "Seismic vibration control of offshore jacket platforms using decentralized sliding mode algorithm", *Ocean Eng.*, **152**, 377-390.

Wahl, A. M. (1944), "Mechanical Springs", The Penton Publishing Company, Cleveland, Ohio.

Wilson, F.J., Bruce, J.M. and Lymon, C.R. (2002), "Dynamics of Offshore Structures", 2nd Ed., Wiley, USA.

Yue, Q. and Bi, X. (2000), "Ice-induced jacket structure vibrations in Bohai sea", *J. Cold Regions Eng.*, **14**(2), 81-92.

Yue, Q., Zhang, Q.L., Zhang, W. and Karna, T. (2009), "Mitigating ice-induced jacket platform vibrations utilizing a TMD system", *J. Cold Regions Sci.Technol.*, **56**(2-3), 84-89.

390 *R.K. Sharma, V. Domala and R. Sharma*

Zhang, B.L. and Han, Q.L.M. (2014), "Network-based modelling and active control for offshore steel jacket platform with TMD mechanisms", *J. Sound Vib.*, **333**, 6796-6814.

MK